

## **ANALYSIS OF PLAIN CONCRETE STRUCTURES BY THE FINITE ELEMENT WITH INNER LINKAGE RODS**

G.Yu, J. Niwa, and T. Tanabe  
Civil Engineering Department, Nagoya University, Japan

### **Abstract**

The numerical implementation of discrete approach is hampered by the need for letting the cracks follow the element boundaries, thereby requiring the introduction of additional nodal points or rearrangement of the original mesh. To overcome this disadvantage, a new method, in which the discrete model represented by rods is embedded into the finite element, is proposed in this paper. The behaviors of the rods are based on the fracture-oriented constitutive relations. Whenever the occurrence of the crack is detected, the general element is replaced by this new element. Also, the objectivity of the method is shown by the analysis of plain concrete structures with different meshes.

Key words: Crack, discrete model, fracture energy, finite element

### **1 Introduction**

Up to now, to describe the cracking of concrete, two different approaches are often used: the discrete approach and the smeared approach. However, there are still some problems existing. The discrete approach is attractive physically, as it reflects the localized nature of cracking, but its numerical implementation is hampered by the need for letting the cracks follow the

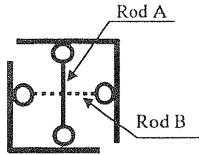


Fig. 1. The rod linkage element

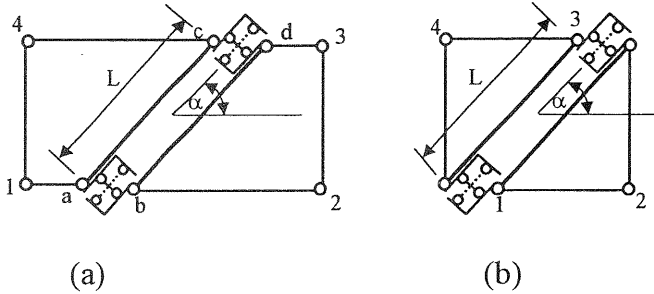


Fig. 2. The element with inner linkage rods

element boundaries, thereby requiring the introduction of additional nodal points or rearrangement of the original mesh. Smeared model has been widely used in finite element analysis. However, for some problems, as pointed out by Rots, J.G.(1988), it is doubtful that the smeared model can suitably simulate the localization of fracture and unloading behaviors in surrounding region for the reason of stress locking.

To overcome the disadvantage of the discrete method, a new method, in which the discrete model represented by rods is embedded into the finite element, is proposed in this paper. The behaviors of the rods are based on the fracture-oriented constitutive relations. Whenever the occurrence of the crack is detected, the general element is replaced by this new element. Also, the objectivity of the method is shown by analysis of plain concrete structures with different meshes.

## 2 Finite element with inner linkage rods

In this research, the rod linkage element is used to represent the localized crack and to link the unloading concrete on two sides of this crack. This rod linkage element is composed of two rods, which follow the fracture-oriented constitutive relation. Figure 1 shows the rod linkage element. Rod A is the rod describing the tensile behavior of the crack and Rod B the shear slip behavior of the crack. Figures 2(a) and 2(b) show the finite element with inner linkage rods when single crack occurs.

The procedure to implement this kind of element can be described as

follows:

1. For every element in the mesh the maximum principle stress at the center of the element is calculated. The stress state at the center of the element can simply be obtained by averaging the stresses at  $2 \times 2$  Gauss points when the 4-node isoparametric element is used, or directly using one-point integration rule. This calculation is repeated at every step of the solution process until the maximum principle stress is equal to or larger than the tensile strength of the material, that means that a crack occurs through the center of the element.
2. From this point on, the finite element where the crack occurs, is replaced by the finite element with inner linkage rods that is mentioned above. The crack with angle  $\alpha$ , shown in Figs. 2(a) and 2(b), is perpendicular to the maximum principle stress. The crack length  $L$  can be calculated and the section area of Rods A and B are equal to  $Lt/2$ , where  $t$  is the thickness of this element. The inner freedom related to points  $a, b, c$  and  $d$  can be eliminated at element level by means of static condensation, by this way the stiffness matrix related with points 1, 2, 3 and 4 can be obtained.

When the crack goes through or near the diagonal nodes of the element, the finite element with inner linkage rods shown in Fig. 2(b) should be used, otherwise the element shown in Fig. 2(a) should be used for ensuring that the element has a good shape and good performance. To use this method to analyze concrete structures, the only thing to do is, first, making a subroutine using displacements control method to describe the nonlinear behaviors of the substructures (shown in Figs. 2(a) and 2(b)), and then, implementing this subroutine into the common used finite element program.

### 3 Fictitious crack model

The fictitious crack model was first introduced by Hillerborg, et al. (1976), and in its original form, it is a discrete approach. When the crack opens the stress is not assumed to fall to zero at once, but to decrease with increasing width, as shown in Fig. 3. At the crack width  $w_1$  the stress falls to zero. Energy dissipated  $D_t$  per unit crack area, is related to the area under the  $\sigma - w$  curve of Fig. 3, i.e.,

$$D_t = \int_0^{w_1} \sigma dw = G_f \quad (1)$$

where  $G_f$  is the fracture energy, i.e., the energy required to create a fully

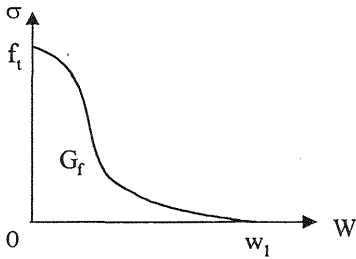


Fig. 3. The fictitious crack model

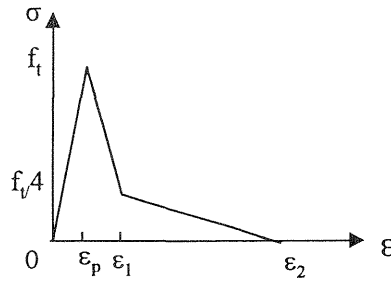


Fig. 4. The stress-strain curve of inner linkage rod A

opened crack plane of unite area.

In the application of the fictitious model, the curve  $\sigma(w)$  may be chosen in different ways. In the analysis of this paper, the curve shown in Fig. 4 is used.

#### 4 Rod element for simulating the tensile behavior of the crack

In Fig. 1, Rod A is used to describe the tensile behavior of the crack.

##### 4.1 Loading behavior

Assuming the rod has the unite length, the loading stress-strain relation curve of Rod A can be shown by Fig. 4. We assume the initial stiffness of the rod element  $E_R = 100 \times E_c$ , where  $E_c$  is the Young's modulus of the concrete, in order to make sure that the difference in displacements at two ends of the rod is small enough before the crack occurs.

The initial stiffness of the rod element  $E_R$  is necessary in the case when the cracks do not occur at the same time on the two sides of the element, for example, for Fig. 2(a), it is possible that the maximum principle stress at the element center and point  $a$  are large than the tensile strength of the concrete while at point  $c$  it is less than tensile strength of concrete.

The strain, stress and tangential stiffness can be expressed as

$$\varepsilon_p = \frac{f_t}{E_R} \quad \varepsilon_1 = 0.75 \frac{G_f}{f_t} \quad \varepsilon_2 = 5 \frac{G_f}{f_t} \quad (2)$$

and

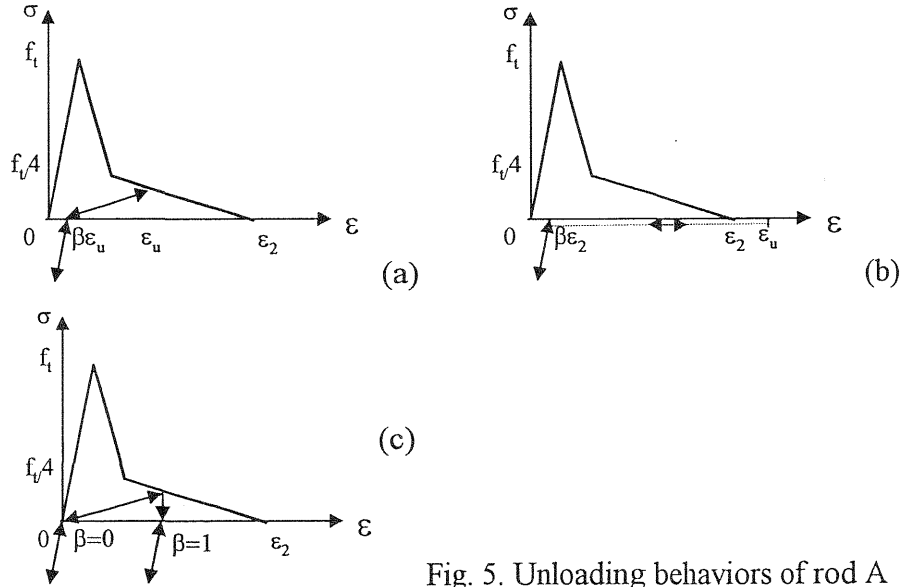


Fig. 5. Unloading behaviors of rod A

$$\sigma = \begin{cases} E_R \varepsilon & 0 < \varepsilon \leq \varepsilon_p \\ f_t - \frac{0.75 f_t (\varepsilon - \varepsilon_p)}{\varepsilon - \varepsilon_p} & \varepsilon_p < \varepsilon \leq \varepsilon_1 \\ \frac{f_t - f_t (\varepsilon - \varepsilon_1)}{4} & \varepsilon_1 < \varepsilon \leq \varepsilon_2 \\ 0 & \varepsilon_2 < \varepsilon \end{cases} \quad (3)$$

$$E = \begin{cases} E_R & 0 < \varepsilon \leq \varepsilon_p \\ -\frac{0.75 f_t}{\varepsilon - \varepsilon_p} & \varepsilon_p < \varepsilon \leq \varepsilon_1 \\ -\frac{f_t}{4(\varepsilon_2 - \varepsilon_1)} & \varepsilon_1 < \varepsilon \leq \varepsilon_2 \\ 0 & \varepsilon_2 < \varepsilon \end{cases} \quad (4)$$

where  $f_t$  is the tensile strength of the concrete and  $G_f$  is the fracture energy of the concrete material.

#### 4.2 Unloading and reloading behaviors

In practice, it is also important to have realistic models for the closing and reopening of cracks, especially when the crack localization phenomenon occurs.

Assume that at point  $(\varepsilon_u, \sigma_u)$ ,  $\varepsilon_p < \varepsilon_u < \varepsilon_2$ , the unloading is detected, the path of unloading will follow the Eq.(5) as shown by Fig. 5(a).

$$\sigma = \begin{cases} \frac{\sigma(\varepsilon - \beta\varepsilon_u)}{(1 - \beta)\varepsilon_u} & \beta\varepsilon_u \leq \varepsilon \\ E_R(\varepsilon - \beta\varepsilon_u) & \varepsilon < \beta\varepsilon_u \end{cases} \quad (5)$$

where  $E_R$  has the same meaning as in Eq. (2). If  $\varepsilon_u > \varepsilon_2$  the unloading and reloading path follow Fig. 5(b).  $\beta$  is the material parameter, if  $\beta$  is chosen as zero, this corresponds to fully recoverable crack width, whereas,  $\beta=1$  corresponds to total irrecoverable crack width as shown in Fig. 5(c). In this study,  $\beta$  is chosen to be 0.

## 5 Rod element for simulating the shear slip behavior of the crack

The original fictitious crack model considers only the behavior of a crack loaded normal to the crack plane. In reality, crack planes are often exposed to shear. From the experimental observation, when the crack occurs, the tangential crack displacement  $w_t$  depends on both the shear stress and the normal crack displacement  $w_n$ . Note that both the Rod A and Rod B have the unit length, we can write

$$\varepsilon_t = f(\tau, \varepsilon_n) \quad (6)$$

where  $\varepsilon_t$  is the strain of Rod B,  $\tau$  is the stress of Rod B and  $\varepsilon_n$  is the strain of Rod A.

For Eq. (6), a simple form as in Ref. (Dahoblom, O. and Ottosen, N.S.(1990)), is used as

$$\varepsilon_t = \frac{\varepsilon_n}{G_s} \tau \quad (7)$$

In order to fit with the experiment results,  $G_s$  is taken as 3.8 Mpa.

## 6 Numerical Example

The purpose of the calculation is not to compare results with experimental evidence, but rather to show that the suggested method can reflect the

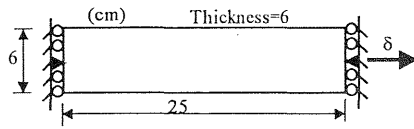


Fig. 6. Dimension and boundary condition of example 1

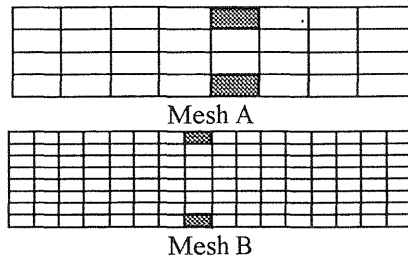


Fig. 7. Meshes used in example 1

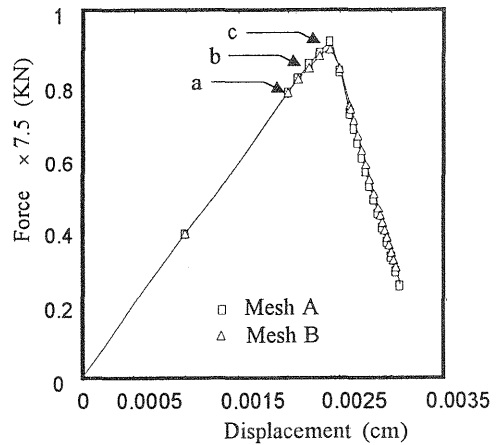


Fig. 8. Load-displacement curves for example 1

localized nature of cracking and is objective in the sense that for decreasing finite element size the total energy dissipated due to cracking approaches the correct value.

For each example, with respect to different load levels, the crack patterns, which indicate the orientation and width of the cracks, are shown. The same magnifying factor is used for all the crack width in the same example, and when the width of the crack is equal to zero (this means the crack has closed), this crack will not be drawn. From these crack patterns, the procedure of opening and closing of the crack can be seen clearly.

### 6.1 Example 1, Uniaxial tension

A plain concrete bar is subjected to prescribed uniform displacements at both ends. The dimension and the supporting conditions are shown in Fig. 6. The material properties are as follows:  $E_c = 21000MPa$ ,  $f_t = 2.63MPa$ ,  $f'_c = 19MPa$  and  $G_f = 100N/m$ .

Two kinds of mesh  $15 \times 8$  and  $8 \times 4$  are used to demonstrate the objectivity of this method and shown in Fig. 7. The imperfection elements, which are shown by the shadow element in Fig. 7 are embedded in the center of two sides of the bar. The imperfection element has the same material properties as the other elements but the thickness is reduced to 3cm.

The load-displacement curves are shown in Fig. 8. Figure 9 depicts the crack patterns at different load levels. The objectivity of this method can be demonstrated by Fig. 8.

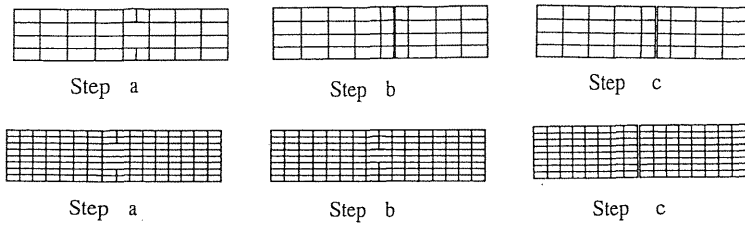


Fig. 9. Crack pattern for example 1

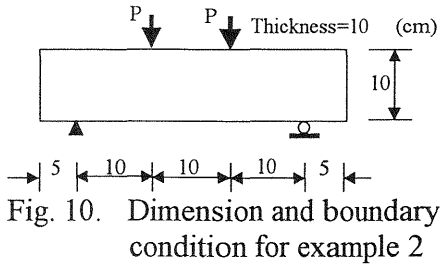


Fig. 10. Dimension and boundary condition for example 2

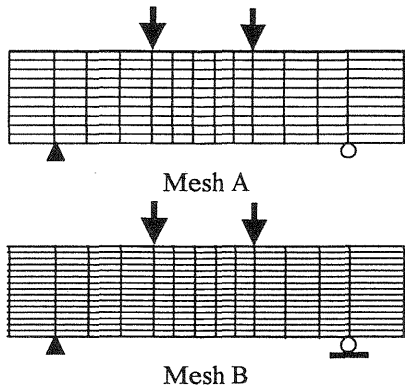


Fig. 11. Meshes used for example 2

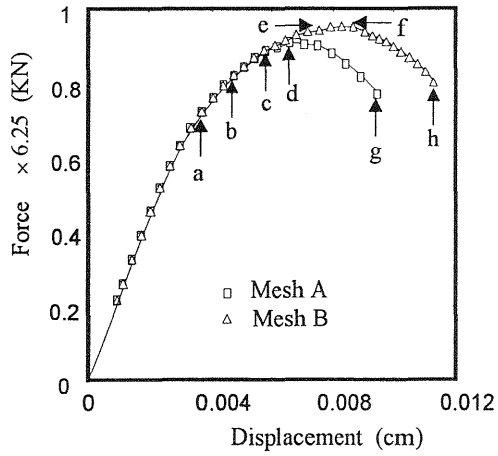


Fig. 12. Load-displacement curves for example 2

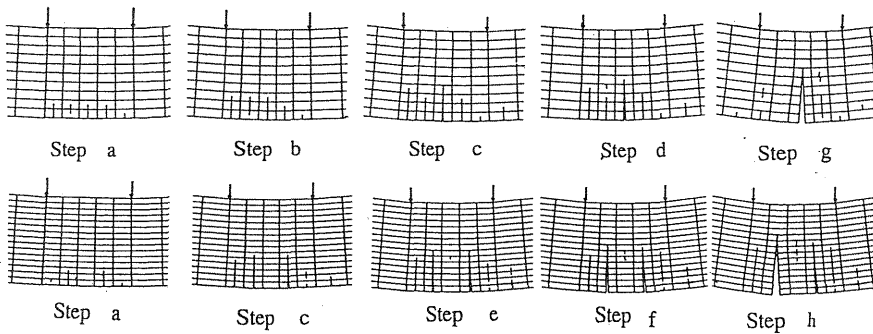


Fig. 13. Crack patterns for example 2

## 6.2 Example 2, Pure bending

The concrete beam geometry is illustrated in Fig. 10. The material properties are the same as these used in section 6.1.

Two kinds of mesh, mesh A and mesh B, are used and shown in Fig. 11. Figure 12 shows the load-displacement curves at the center of the lower side of the beam for mesh A and B, respectively. Corresponding to the steps marked in Fig. 12, the crack patterns are shown in Fig. 13.

For this particular problem, at the same depth of the beam between the two point loads, the stress states are the same, and cracks can occur at the same time. After cracks occur, the procedures of crack opening or crack closing takes place. The opening of crack can be in one element, two elements or more. It is a bifurcation phenomenon. For uniaxial tensile problem, the bifurcation path affects the post-peak response of the specimen causing different post-peak load-displacement curves, but the values of the peak points are the same. For this pure bending case, since the bifurcation phenomenon occurs before the peak point, the bifurcation path affects not only the post-peak response of the specimen, but also the pre-peak response, including the value of the peak point. Without any imperfection (like in section 6.1), the path can not be pre-determined. So, they're big difference between the two load-displacement curves corresponding to different meshes.

## 6.3 Example 3, Shearing

The plain concrete wall is subjected to shear displacement as illustrated in Fig. 14. A series of computation are carried out with uniformly designed finite element (4 by 4, 6 by 6 and 8 by 8). The inherent objectivity of the numerical results with respect to the choice of the finite element mesh is reasonably well demonstrated in Fig. 15. The progressive development of cracks with regard to different stages is depicted in Fig. 16.

## 7 Conclusions

In this paper, a method to model the crack behaviors of concrete is presented, where the crack inside the element is represented by two rod elements whose behavior is based on the fracture-oriented constitutive relations. Unlike the discrete model, this method does not require rearrangement of the original mesh or predefined crack. But there are still some problems needed to be solved: (1) for certain cases, as shown in example 3, on the final stage when the specimen fail, a continuous crack can not be formed by individual cracked element, (2) the relation between the nodal force and the nodal displacement of the element with inner linkage rods (Fig. 2) is obtained by subroutine (a sub nonlinear program), instead of simple equations.

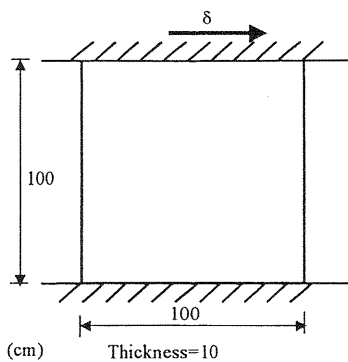


Fig. 14. Dimension and boundary curves Condition for example 3

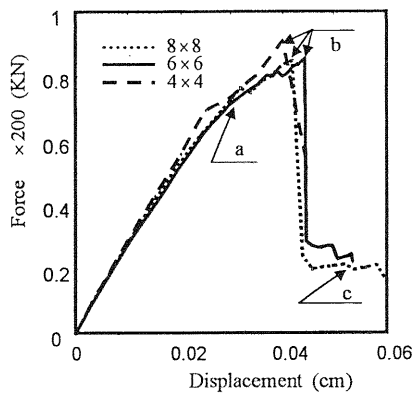


Fig. 15. Load-displacement curves f or example 3

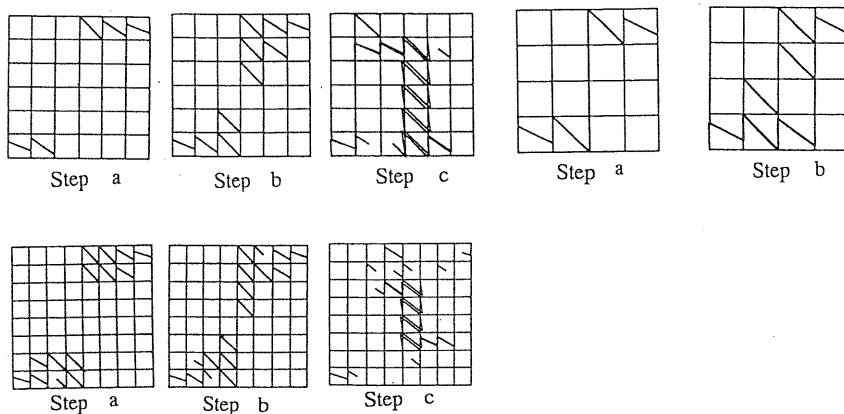


Fig. 16. Crack patterns for example 3

## 8 References

- Dahoblom, O. and Ottosen, N.S. (1990) Smearred crack analysis using generalized fictitious crack models. **ASCE Journal of engineering mechanics**, 116(1), 55-76.
- Hillerborg, A., Mod er, M. and Petersson, P.E. (1976a) Analysis of crack formation and crack growth in concrete by means of fracture mechanics and finite elements. **Cem. & Concr. Res.**, 6, 773-782.
- Rots, J.G. (1988) Computational modeling of concrete fracture, **Heron**, 34(1), 59.